

5.1 IRRADIATION RESPONSE OF NEXT GENERATION HIGH TEMPERATURE SUPERCONDUCTING RARE-EARTH AND NANOPARTICLE-DOPED $\text{YBa}_2\text{Cu}_3\text{O}_{7-x}$ COATED CONDUCTORS FOR FUSION ENERGY APPLICATIONS — K. J. Leonard, T. Aytug, F. A. List, III, (Oak Ridge National Laboratory); A. Perez-Bergquist, W. J. Weber, (University of Tennessee); and A. Gapud (University of South Alabama)

OBJECTIVE

The goal of this work is to evaluate the irradiation response of the newest generation of coated conductors based on rare earth and nanoparticle doping of the $\text{YBa}_2\text{Cu}_3\text{O}_{7-x}$ (YBCO) high temperature superconductor. The materials under investigation represent different methods for enhanced flux pinning for improved performance under externally applied magnetic fields. Ion beam irradiation will be used to simulate neutron damage cascades in the materials to examine the effect that radiation damage has on the different pre-existing defect structures used for flux pinning and to evaluate the superconductors capability for use in fusion reactor systems.

SUMMARY

The irradiated superconducting properties of Zr-doped $(\text{Y,Gd})\text{Ba}_2\text{Cu}_3\text{O}_{7-x}$, $(\text{Dy,Y})\text{Ba}_2\text{Cu}_3\text{O}_{7-x}$ and $\text{Gd}_2\text{Ba}_2\text{Cu}_3\text{O}_{7-x}$ are being evaluated for 5 MeV Ni, and 25 MeV Au irradiations to fluences between 10^{11} and 10^{12} ions/cm². For low fluence irradiations, small decreases were observed in the critical current for a-b pinning in both the $\text{GdBa}_2\text{Cu}_3\text{O}_{7-x}$ and $(\text{Dy,Y})\text{Ba}_2\text{Cu}_3\text{O}_{7-x}$ conductors, but increased pinning at other angular orientations, decreasing angular field isotropy. The 10^{12} cm⁻² 25 MeV Au irradiated $(\text{Dy,Y})\text{Ba}_2\text{Cu}_3\text{O}_{7-x}$ did show a reduction in critical current, J_c , for externally applied magnetic fields of less than 7 Tesla for tests conducted at 77 K. However, at higher field strengths the irradiated J_c values exceed that of the unirradiated material. Properties of the Zr-doped $(\text{Y,Gd})\text{Ba}_2\text{Cu}_3\text{O}_{7-x}$ conductor also show positive results following low fluence 5 MeV Ni and 25 MeV Au irradiation, where increases in a-b pinning are observed over the control samples.

PROGRESS AND STATUS

Introduction

During the first half of the year, work has been performed in examining the ion irradiation response of the three advanced high temperature-superconducting (HTS) tapes. The HTS materials under examination include Zr-doped $(\text{Y,Gd})\text{Ba}_2\text{Cu}_3\text{O}_{7-x}$, $(\text{Dy,Y})\text{Ba}_2\text{Cu}_3\text{O}_{7-x}$ and $\text{Gd}_2\text{Ba}_2\text{Cu}_3\text{O}_{7-x}$. The supplied Zr-doped $(\text{Y,Gd})\text{Ba}_2\text{Cu}_3\text{O}_{7-x}$ and $(\text{Dy,Y})\text{Ba}_2\text{Cu}_3\text{O}_{7-x}$ conductors had critical current, I_c , values in self-field of approximately 239 A/cm-width and 525 A/cm-width over 1 meter length of tape, respectively. These tapes have been cut down into smaller test samples. The purchased $\text{Gd}_2\text{Ba}_2\text{Cu}_3\text{O}_{7-x}$ tape was already pre-cut into ~ 1 inch test samples. Patterned current bridges were laser scribed into the HTS test samples for electrical characterization in order to accommodate the high current samples on the available measurement equipment. Silver was deposited at specific sites for the pad positions of the four-probe voltage and current contacts. Following this, the samples were given a thermal anneal in oxygen at 500°C for 1 hour. Ion irradiations at the University of Tennessee Ion Beam Materials Laboratory were performed on the samples at and around the electrical bridge location where the Ag contact is not present. Beam penetration through the Ag contact is not considered due to the >2mm thickness of the Ag layer.

Irradiations to date include 25 MeV Au to fluences of $1 \times 10^{11} \text{ cm}^{-2}$ and $1 \times 10^{12} \text{ cm}^{-2}$, and 5 MeV Ni to $5.5 \times 10^{11} \text{ cm}^{-2}$. The low ion energies were selected to produce defect cascades similar to that observed in neutron irradiations rather than ion track formation, while being energetic enough to produce implantation only in the Ni-base substrates. The fluence of the 5 MeV Ni was selected to match damage levels of the lower fluence 25 MeV Au irradiations in the material as estimated through TRIM calculations. The high fluence of the 25 MeV Au irradiation was estimated to be near the peak damage level of the films prior to degraded properties, based on ion irradiation studies of $\text{YBa}_2\text{Cu}_3\text{O}_{7-x}$ films using different ion and energy ranges by Hensel and coworkers [0]. Pre and post-irradiation electrical characterization was performed at both ORNL and University of South Alabama (USA). The work performed at ORNL consisted of angular field dependency of critical current (I_c vs. ϕ) for applied fields up to 1.5 Tesla at 77 K. Measurement of critical temperature, T_c , resistivity versus temperature and critical current, J_c , as a function of magnetic field were done at USA. Microstructural characterization was performed at ORNL by transmission electron microscopy (TEM) through focus ion beam processing of TEM specimens.

Less than 1 K change in the T_c of the superconducting samples was measured for the 10^{11} cm^{-2} 25 MeV Au irradiated samples as compared to that of the unirradiated control. Values of T_c were reduced between 4 and 6 K from the unirradiated values (92.4 to 93.4 K) following irradiation to the higher fluences ($1 \times 10^{12} \text{ cm}^{-2}$, 25 MeV Au). The reduction in T_c is similar to the effects of oxygen deficiency within the conductor [0].

The current progress of work is outlined in

Table 1 for the three HTS sample types. The 25 MeV Au irradiated samples have completed or are nearing completion of their electrical characterization, but the more recent 5 MeV Ni irradiated specimens are beginning testing at the time of writing this report. Furthermore, some specific retesting of samples is being performed to confirm data (marked as R in the table), or to replace a sample that had shown a large defect in the film layer (marked as S in the table). While microstructural characterization of the 25 MeV Au samples has been completed, characterization of the 5 MeV Ni samples is pending on results of electrical characterization.

The $\text{GdBa}_2\text{Cu}_3\text{O}_{7-x}$ conductor

The pre-irradiated microstructure (see winter 2012 Fusion semi-annual report for details of microstructures of all unirradiated HTS materials) of the $\text{GdBa}_2\text{Cu}_3\text{O}_{7-x}$ (GdBCO) conductor contained a significant amount of anti-phase domain boundaries as well as $\text{Gd}_2\text{BaCuO}_4$, or Y211 type intergrowths in the film structure. The amount of intergrowths appeared to be significantly greater than that observed in the other HTS types examined in this work. Furthermore, the GdBCO film contained small (3.8 nm average size) particles of Gd_2O_3 distributed evenly, but with some ordering along the a-b directions in the film.

A comparison of the microstructures developed on irradiation is shown in Figure 1. Irradiation of the GdBCO film by 25 MeV Au resulted in the observed reduction in length of the anti-phase domain boundaries extending up from the buffer layer interface. While this may suggest some healing of the structure, it can reduce effective pinning centers as well as sources for intergrowths, which can improve electrical properties (flux pinning) under external magnetic fields. Radiation induced defects visibly appear in the microstructure by $1 \times 10^{12} \text{ cm}^{-2}$. These defects were on the order of only a couple nanometers in size and consisted of localized lattice disorder. However, the strain within the GdBCO lattice from these defects produce lobe-type diffraction contrast through the interaction with the beam electrons of the microscope that makes these defects easily visible at lower magnifications. The irradiated samples also showed an even mixture of Y211 and $\text{GdBa}_2\text{Cu}_4\text{O}_8$ (Y124) type intergrowths, while only Y211 were

identified in the unirradiated control. It is not clear at this time how this may influence the electrical properties of the film, but suggests some chemical ordering in the matrix resulting in increased Ba-Cu in the intergrowths. Another observed change in the irradiated microstructure is the disappearance of the Gd_2O_3 particles within the film following 25 MeV Au fluences above $1 \times 10^{11} \text{ cm}^{-2}$.

Table 1. Summary of ion irradiation work to date on the HTS conductors, with electrical work performed at ORNL and University of South Alabama (USA).

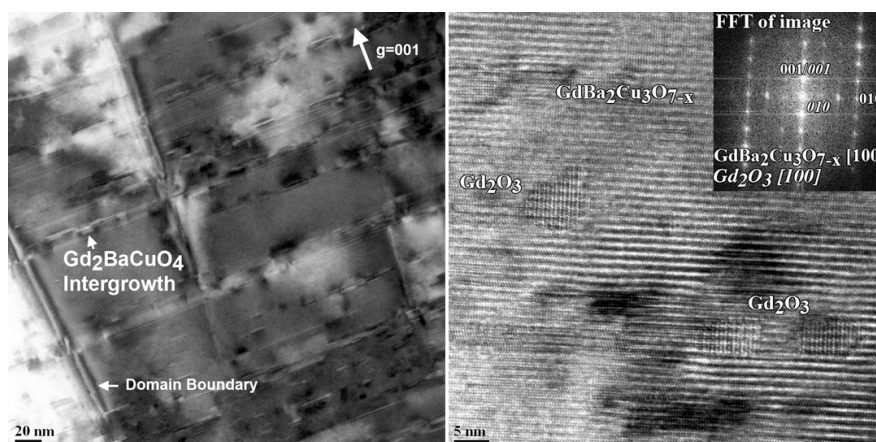
HTS type	Ion Irradiation Conditions	Electrical		Microstructural
		ORNL	USA	
$\text{GdBa}_2\text{Cu}_3\text{O}_{7-x}$	25 MeV Au, $1 \times 10^{11} \text{ cm}^{-2}$	C	M	C
	25 MeV Au, $1 \times 10^{12} \text{ cm}^{-2}$	C	C	C
	5 MeV Ni, $1 \times 10^{11} \text{ cm}^{-2}$	C	M	P
$(\text{Dy}, \text{Y})\text{Ba}_2\text{Cu}_3\text{O}_{7-x}$	25 MeV Au, $1 \times 10^{11} \text{ cm}^{-2}$	R	C	C
	25 MeV Au, $1 \times 10^{12} \text{ cm}^{-2}$	S	C	C
	5 MeV Ni, $1 \times 10^{11} \text{ cm}^{-2}$	C	M	P
$\text{Zr-YBa}_2\text{Cu}_3\text{O}_{7-x}$	25 MeV Au, $1 \times 10^{11} \text{ cm}^{-2}$	C	C	C
	25 MeV Au, $1 \times 10^{12} \text{ cm}^{-2}$	M	M	M
	5 MeV Ni, $1 \times 10^{11} \text{ cm}^{-2}$	C	M	P

C = completed, M = currently being measured/examined, P = pending, S = second sample being tested, R = sample being remeasured to confirm properties.

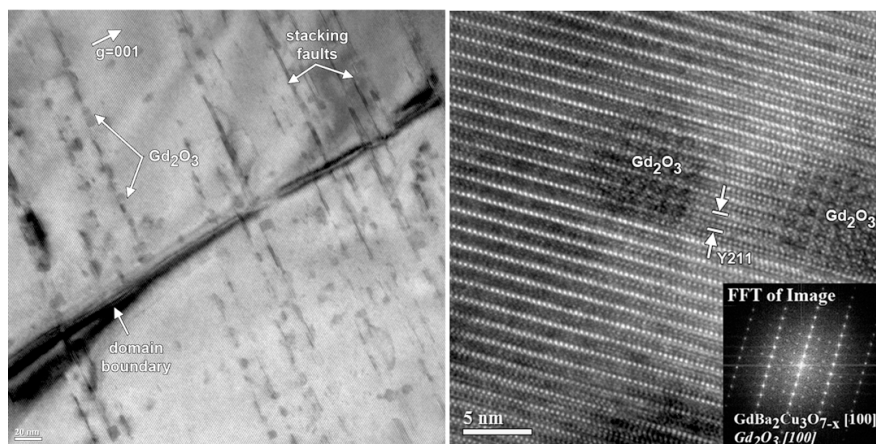
Similar responses in electrical transport properties were observed for the 5 MeV and low dose 25 MeV Au irradiations (Figure 2a), which were irradiated to equivalent damage levels. For the 1 T applied magnetic field in the H//ab direction ($\phi=0^\circ$), a slight reduction in the I_c is observed. However, increased critical currents through enhanced pinning are observed throughout the other angles. Irradiation to higher doses, 25 MeV Au at $1 \times 10^{12} \text{ cm}^{-2}$, results in the suppression of a-b axis pinning with little damage to the superconductor as noted by the equivalent response at higher applied angles to that of the unirradiated control. This effect is seen in plotting of I_c versus applied magnetic field (Figure 2b), where the sample currents of the lower fluence irradiations increase over the unirradiated values at fields of 0.3 T and higher. The loss in pinning associated with the high fluence 25 MeV Au irradiation is evident in both the diminished H//ab peak suggesting a significant effect that the changing structure of the intergrowths and loss of Gd_2O_3 particles have on the overall property of the films.

Reduced values of J_c are measured for higher magnetic fields (Figure 2c), which suggest limited effects of the radiation-induced defects on pinning properties. While the loss in J_c can be associated with consolidation of cascade damage resulting in regions of amorphous material that begin to interlink [0,0], the microstructure of the irradiated film did not show this. Furthermore, no decrease in I_c was observed in the high fluence irradiations for the H//c condition. Therefore, the loss in J_c of the high dose 25 MeV Au irradiations is due to the loss of pinning rather than accumulated damage in the superconductor. The J_c vs applied field data for the low fluence irradiations remains to be tested, but should show greater currents than the unirradiated control at high fields. While J_c values at high H fields are low, this can be increased through reductions in measurement temperatures.

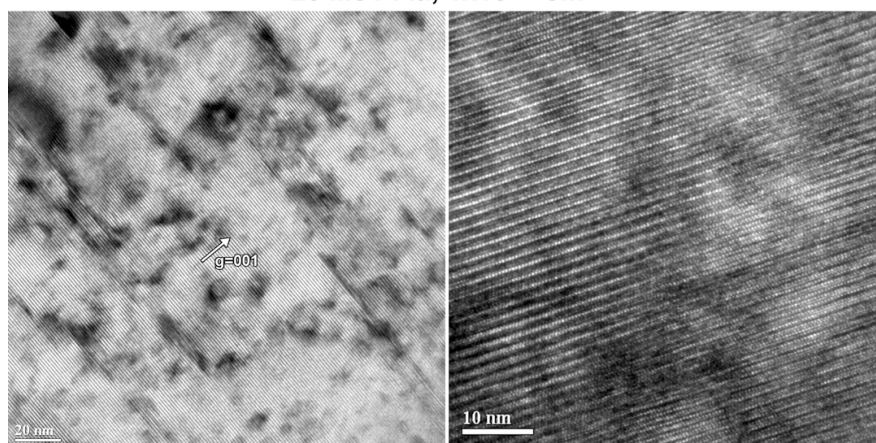
Critical temperature, T_c , of the $1 \times 10^{11} \text{ cm}^{-2}$ 25 MeV Au irradiated GdBCO films showed a small decrease with respect to the unirradiated control (93.4 versus 93.2 K) and is within the error of the measurement. However, the $1 \times 10^{12} \text{ cm}^{-2}$ 25 MeV Au irradiated showed a decrease in T_c to 87.3 K.



Control



25 MeV Au, 1x10¹¹ cm⁻²



25 MeV Au, 1x10¹² cm⁻²

Figure 1. Comparison of the changes in the microstructure of the GdBa₂Cu₃O_{7-x} conductor with 25 MeV Au irradiation. Micrographs taken from low and higher magnifications to illustrate the development of visible radiation induced defects and the disappearance of Gd₂O₃ particles by 1x10¹² cm⁻².

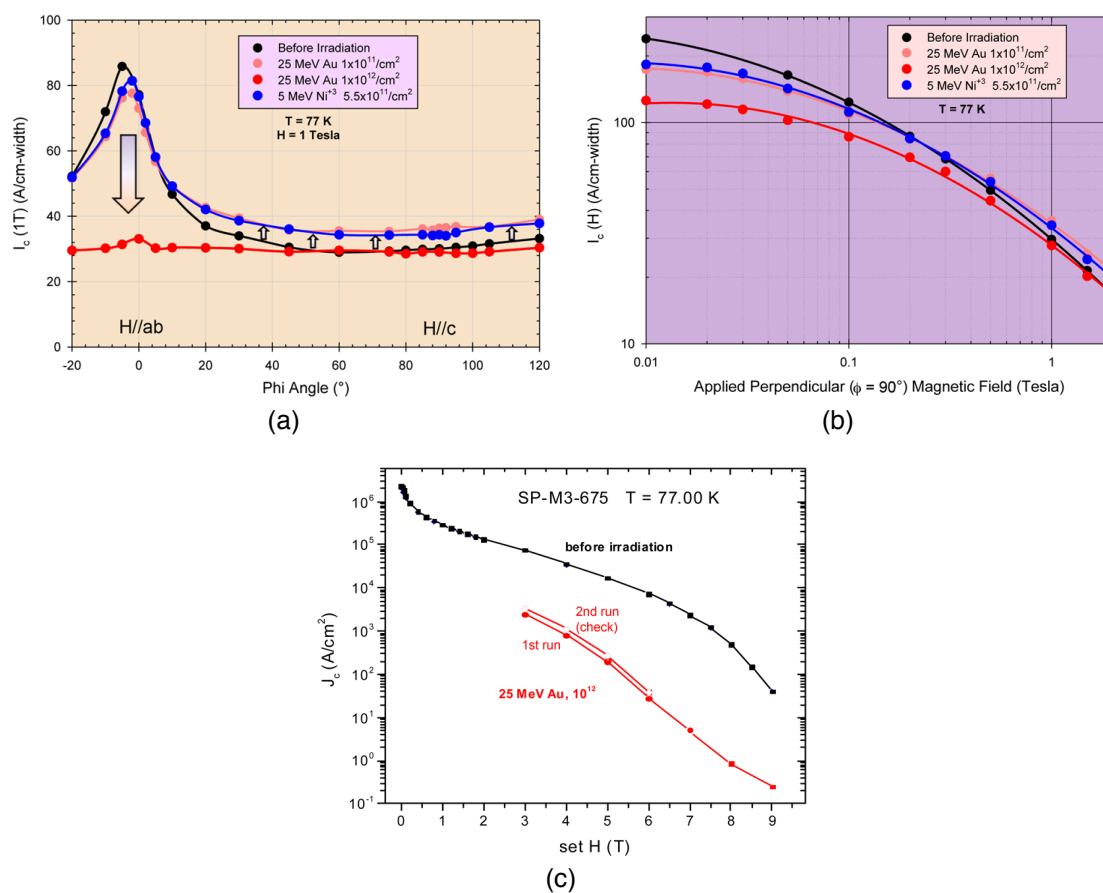


Figure 2. Changes in electrical property of GdBa₂Cu₃O_{7-x} conductor following irradiation by 5 MeV Ni and 25 MeV Au ions. (a) Angular dependence of critical current showing substantial decrease in a-b pinning in the high fluence irradiations, but improvements overall pinning at lower fluences. (b) Critical current as a function of magnetic field to 1.5 T for the H//c condition of the data shown in (a), and (c) the critical current density as a function of applied field to 9 T for the high fluence 25 MeV Au irradiation compared to the control. The J_c vs field data for the lower dose samples remain to be tested.

The (Dy,Y)Ba₂Cu₃O_{7-x} conductor

Very little difference was observed between the pre-irradiated and post irradiated microstructures of the (Dy,Y)Ba₂Cu₃O_{7-x} conductor (DyBCO). Examples of the microstructures are shown in Figure 3. The microstructure of the 1x10¹¹ cm⁻² 25 MeV Au irradiated material was found to be indistinguishable with the unirradiated control and is not shown in the figure. Average (Dy,Y)₂O₃ particles size and density measured in the irradiated and unirradiated samples were found to be statistically unchanged with values around 26 nm and 4.7x10²¹ m⁻³, respectively. Intergrowths in the control and irradiated samples were typically found to be Y124 type, assuming that Dy is also substituting for Y in these layers as well. Similar to the previously discussed GdBCO, visible radiation-induced defects in the DyBCO sample do not begin to appear in the TEM samples until a dose of 1x10¹² cm⁻² 25 MeV Au. However, in

addition to the small (~ 2 nm) defects that appear as localized disorder in the stacking sequence of the conductor in the high dose sample, there are also larger (~ 5 nm) defects that are amorphous in structure. The amorphous defects are very few in number (too few to obtain statistics), and do not show the strain contrast surrounding them as the smaller defects show. The 1×10^{12} cm $^{-2}$ 25 MeV Au irradiated DyBCO sample was the only sample to show the amorphous defect features.

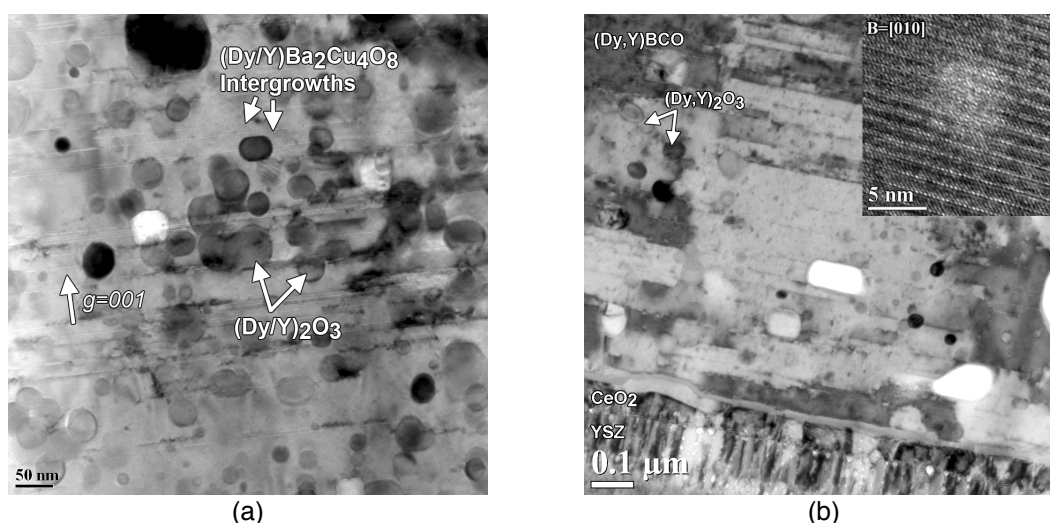


Figure 3. Micrographs of (Dy,Y)Ba₂Cu₃O_{7-x} (a) control and (b) 1×10^{12} cm $^{-2}$ 25 MeV Au irradiated samples. The speckling appearing in the irradiated sample are radiation-induced defects. The insert of (b) shows a larger radiation-induced defect in the conductor consisting of an amorphous sphere.

Irradiation to 5.5×10^{11} cm $^{-2}$ 5 MeV Ni was found to decrease the H//ab pinning in the conductor, but generally increases pinning over other angular field directions (Figure 4). Therefore, reducing the anisotropy of the sample, which in itself can be a positive effect in terms design flexibility for these conductors in applications. For H//c conditions, the 5 MeV Ni irradiated films show higher I_c values with increasing magnetic field starting at 0.5 T. The sample irradiated to 1×10^{12} cm $^{-2}$ by 25 MeV Au showed a significant loss in the I_c over all angular field measurements for the 1 T condition. A retesting of this sample will be performed to verify this. Comparatively, a second sample tested at USA for field dependence of J_c (Figure 4c) did not show as significant of a loss as the sample that ORNL retained for angular dependence tests. For the field dependence study, the high dose 25 MeV irradiated sample shows a cross-over point with the unirradiated condition, in which higher J_c values are found in the irradiated material above 7 T for the samples tested at 77 K. The lower dose, 1×10^{11} cm $^{-2}$, Au irradiated sample showed consistently higher J_c values over that of the unirradiated values (of which are from the same sample in the pre-irradiated condition).

While defects are not visible in the lower dose irradiation, which may consist of lattice site disorder in the conductor, they do contribute to improved properties of the conductor with irradiation. For the DyBCO sample, the high dose irradiated material does show some loss in conduction under low applied fields, but demonstrates improved high field pinning from the defects generated. The 5 MeV Ni irradiated samples are currently undergoing field

dependence, irreversibility and T_c testing at USA. Furthermore, the lower dose 25 MeV Au irradiated sample retained by ORNL for testing requires a second sample to be tested as the first sample showed a visible crack at the bridge location of the sample.

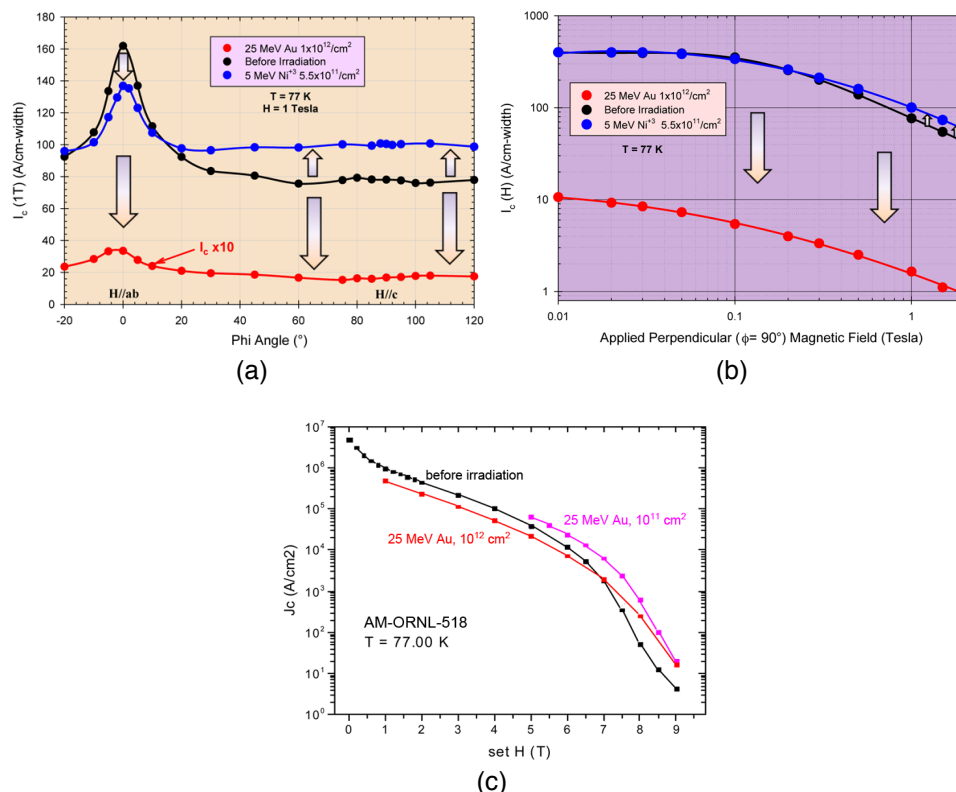


Figure 4. Changes in electrical property of (Dy,Y)Ba₂Cu₃O_{7-x} conductor following irradiation by 5 MeV Ni and 25 MeV Au ions. (a) Angular dependence of critical current showing dramatic loss in sample irradiated to $1 \times 10^{12} \text{ cm}^{-2}$ 25 MeV Au, while increased pinning observed in the 5 MeV Ni irradiated material. (b) Critical current as a function of magnetic field to 1.5 T for the H//c condition of the data shown in (a), and (c) the critical current density as a function of applied field to 9 T for the 25 MeV Au irradiations compared to the control. A retesting of the angular field dependence of the 25 MeV Au sample, shown in (a), is planned to confirm the result.

The change in T_c with irradiation for the low fluence 25 MeV Au irradiated sample was within a degree of the unirradiated control (92.4 K). The higher fluence 25 MeV Au irradiation resulted in a reduction of T_c to 87.9 K. This was less of a change as compared to the high fluence 25 MeV irradiated GdBCO sample.

The Zr-doped YBa₂Cu₃O_{7-x} conductor

At this time the microstructure of only the control and the $1 \times 10^{11} \text{ cm}^{-2}$ 25 MeV Au irradiated Zr-doped (Y,Gd)Ba₂Cu₃O_{7-x} (Zr-YBCO) sample has been examined. The irradiated material shows a substantial difference in comparison to the microstructure of the unirradiated control (Figure 5). A significant change in the size and distribution of the BaZrO₃ (BZO) particles is observed following irradiation, in which the

length of the c-axis oriented chains of BZO particles is dramatically reduced by as much as 25% in the c-axis direction. While the width of the BZO particles is relatively unchanged and averages 8 nm. Furthermore, the aligned BZO particle chains show a distinctive and orderly spacing in the irradiated material as compared to a more random distribution in the control. However, the thickness of the irradiated TEM specimen was a little thinner than that of the control, and may account for some of the spatial differences observed between the irradiated and control specimens.

Another difference observed between the control and irradiated Zr-YBCO microstructure is that the conductor immediately around the BZO particles is more faulted in the irradiated material. However the extension of the faults, or intergrowths, into the matrix does not frequently occur. In fact the length of the intergrowths in the control appears longer than those in the irradiated material, but further statistical analysis is required. The irradiated microstructure show Y124 type intergrowths exclusively, compared to a mixture of Y211 and Y124 observed in the control material.

Electrical characterization testing at ORNL has been completed on the $1 \times 10^{11} \text{ cm}^{-2}$ 25 MeV Au and $5.5 \times 10^{11} \text{ cm}^{-2}$ 5 MeV Ni irradiations; the higher fluence 25 MeV Au irradiations still remain to be completed. Shown in Figure 6, an increase in a-b pinning is observed following irradiation with no decrease in I_c for the H//c condition. While the length of the BZO particles in the c-axis direction is reduced, this was not significant enough to create any reduction in the effectiveness of pinning in the H//c condition. The increased H//ab pinning may be related to either the increased point defects in the conductor or the increased faults present at the BZO particle interfaces. As the Zr-YBCO sample is the only conductor in this study to show a rise in the H//ab pinning with irradiation, the faults at the BZO samples are more likely to be the contributor.

The T_c value of the $1 \times 10^{11} \text{ cm}^{-2}$ 25 MeV Au irradiated Zr-YBCO sample only decreased by 0.6 K over that of the unirradiated control.

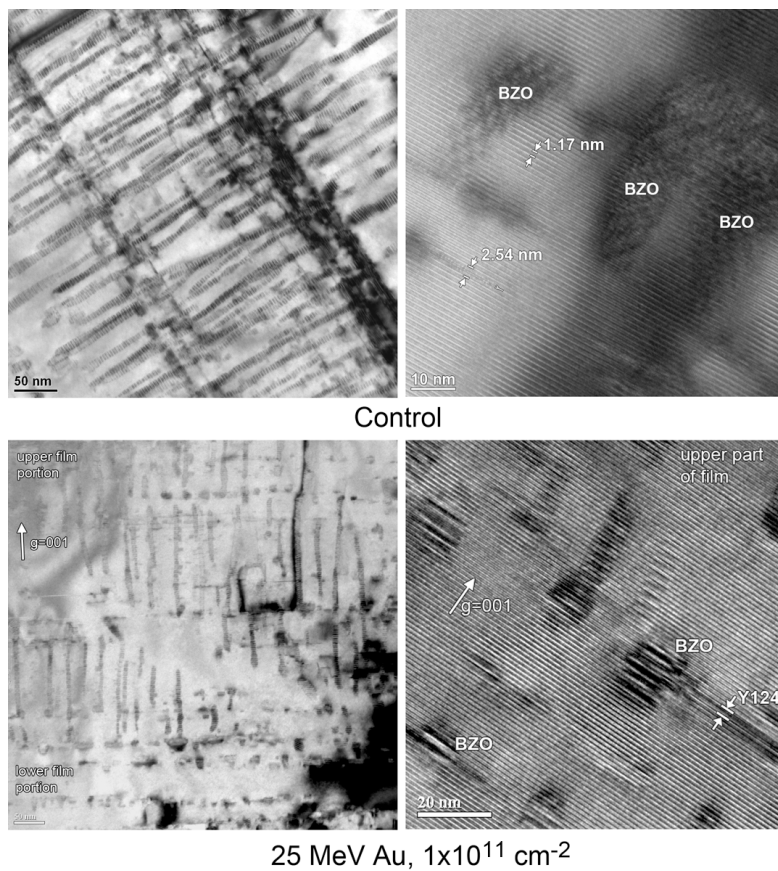


Figure 5. Comparison micrographs of Zr-doped $(Y,Gd)Ba_2Cu_3O_{7-x}$ in the unirradiated and 25 MeV Au irradiated conditions, showing the decrease in $BaZrO_3$ particle chain lengths in the c-axis direction of the conductor and in the increased localized faulting around the particles in the irradiated material.

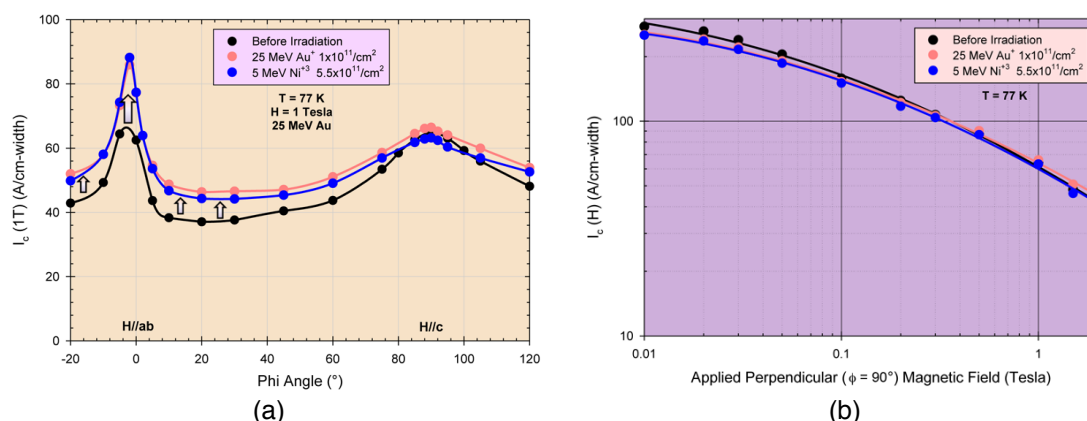


Figure 6. Comparison of 5 MeV Ni and 25 MeV Au irradiation to similar damage levels in Zr-doped (Y,Gd)Ba₂Cu₃O_{7-x} to that of the control sample. (a) Angular dependence of I_c in a 1 T field at 77 K, and (b) a replot of I_c versus field for the H//c condition comparing the samples.

CURRENT AND FUTURE WORK

Continued testing of ion irradiated samples both at ORNL and USA will progress, based on the needed information to complete the gaps shown in Table 1. This will include the full electrical characterization of the irradiated HTS conductors. Some follow up microscopy may be performed to verify or address uncertainties based on analysis of electrical characterization. Additional structural characterization may be performed on the irradiated conductors that could include energy electron loss spectroscopy using the TEM, or Raman spectroscopy in evaluating the local bonding and changes within the conductors resulting from radiation induced damage. Further evaluation of possible in situ testing of the HTS materials under ion irradiation will also begin to be considered.

REFERENCES

- [1] R. Feenstra, D. K. Christen, J. D. Budai, S. J. Pennycook, D. P. Norton, D. H. Lowndes, C.E. Klabunde and M. D. Galloway, "Properties of Low Temperature, Low Oxygen Pressure Post-annealed YBa₂Cu₃O_{7-x} Thin Films, in High T_c Superconductor Thin Films," L. Corraera ed., Elsevier Science Publishers (1992) 331.
- [2] B. Hensel, B. Roas, S. Henke, R. Hopfengartner, M. Lippert, J. P. Stobel, M. Vildic and G. Saemann-Ishenko, *Phys. Rev B* **42** 7, (1990) 4135.
- [3] M. A. Kirk and Y. Yan, *Micron* **30** (1999) 507-526.
- [4] J. R. Liu, J. Kulik, Y. J. Zhao and W. K. Chu, *Nucl. Instrum. Methods Phys. Res. B* **80/81** (1993) 1255.